Combustion Theory and Modelling, 2019
Vol. 23, No. 5, 798–820, https://doi.org/10.1080/13647830.2019.1589581

Flame Balls in a non-uniform reactive mixture: preferential diffusion, heat-loss and stability

Joel Daou[a*] and Remi Daou[b]

[a]*School of Mathematics, University of Manchester, Manchester, UK;* [b]*Faculté d'ingénierie-ESIB, Université Saint-Joseph, Beirut, Lebanon*

(*Received 17 December 2018; accepted 26 February 2019*)

The paper examines the existence and stability of axisymmetric flame balls in a non-uniform reactive mixture corresponding to a mixing layer taking into account preferential diffusion and volumetric heat-loss. The mixture's non-uniformity is measured with a non-dimensional parameter ϵ which is inversely proportional to the square root of the Damköhler's number. The investigation is carried out analytically in the limit of large activation energy and small values of ϵ, and numerically in the general case. New simple formulas accounting for preferential diffusion are derived which determine in particular the thermal energy and location of the flame ball; these may be argued to represent the minimum ignition energy and optimum spark location for a successful forced ignition of the diffusion flame in the mixing layer. A new free boundary problem (FBP) with two dependent variables is derived which describes non-adiabatic flame balls subject to volumetric heat-loss from the burnt gas. For small ϵ, the analytical solution to the FBP shows that the main effect of weak non-uniformity can be understood in a simple way if the volume of the distorted flame ball is characterised by an equivalent radius $R_{\rm eq}$ which is plotted versus a heat-loss parameter κ. Specifically, the curve $R_{\rm eq}(\kappa)$ is the same inverse-C shaped curve found in the literature in the uniform case ($\epsilon = 0$) but shifted to the left by an amount, proportional to ϵ^2, which explicitly accounts for all parameters. The numerical investigation addresses the existence of the axisymmetric flame balls and their stability within two models familiar in studies on flame balls in uniform mixtures, namely the 'far-field losses model' where heat-losses from the burnt and unburnt gas are accounted for, and the 'near-field losses model' adopted in our analytical investigation, where heat-loss from the unburnt gas is neglected. Typically four regions are determined in the κ-ϵ plane for fixed Lewis numbers which identify conditions for the existence of either the flame ball, the diffusion flame or of both. This subdivision is argued to provide useful insight regarding the possible modes of burning in the mixing layer. A particularly interesting type of solutions identified for moderate values of ϵ corresponds to ring-shaped flame balls, termed 'flame rings', in regions where the diffusion flame cannot exist. As for the stability of the flame balls, we have found these to be typically unstable, as expected for their spherical counterparts. However, we have also determined these to be stable in special circumstances requiring low Lewis numbers and the presence of heat-losses and depending on the non-uniformity parameter ϵ. Furthermore, an increase in ϵ was found to play a stabilising effect, at least for the cases considered.

Keywords: ignition of diffusion flames; ignition in non-uniform mixtures; flame balls; flame stability

*Corresponding author. Email: joel.daou@manchester.ac.uk

1. Introduction

The problem of flame ignition in a non-uniform reactive mixture by a localised energy deposit is ubiquitous in combustion applications. This situation is typically encountered in the forced ignition of a diffusion flame, by means of a spark say, after the mixing of reactants has occurred in a mixing layer. Surprisingly, the fundamental question of determining the critical conditions for successful ignition in a reactive mixing layer has not received dedicated attention in the literature. To address this question, a theoretical model was derived and investigated analytically and numerically in two of our recent publications [1, 2]. One important objective of these publications was to determine the critical minimum ignition energy and the optimum location for its deposit. These were argued to be related, in first approximation, to the thermal energy inside a non-propagating non-spherical axisymmetric structure, termed flame ball, generalising the well known spherical Zeldovich flame ball to non-uniform mixtures. This stationary axisymmetric flame ball is typically expected to be unstable, as it is the case with its spherical counterpart in uniform premixed gases [3, p. 327]. In fact, the inherent instability of flame balls does not diminish their importance at all, since it may be viewed as an essential ingredient for characterising the 'critical conditions' for successful ignition in any theoretical analysis following the pioneering interpretation of Zeldovich [4]. It has been found experimentally however that stable spherical flame balls can be observed at zero gravity if the Lewis number of the deficient reactant is small enough [5]. Theoretical models have explained the existence of such stable spherical flame balls in special circumstances where preferential-diffusion and heat-losses are taken into account [6–13]. An additional mechanism promoting stability has been identified to be associated with the presence of a drift velocity, with the existence of apparently stable drifting flame balls having been demonstrated theoretically, numerically, and experimentally [14–19]. For the non-spherical flame balls in a non-uniform mixture considered in [1, 2], the effect of preferential-diffusion and heat-loss and the flame stability have not been investigated, although these aspects are essential to complete the model.

In this paper, we shall complement the findings of [1, 2] with new results addressing the effects of preferential-diffusion and heat-loss on the existence and stability of the axisymmetric flame balls. Analytical results will be derived in the large Damköhler's number limit (or small values of a non-dimensional parameter ϵ) for the shape of the flame ball and its location; these may be used to assess the minimum energy required for successful ignition and the optimum location for its deposit. The optimum location is in fact only relevant in non-uniform mixtures as considered herein and, as we shall see, it needs not coincide with the stoichiometric location as an educated guess may suggest. Two models accounting for heat-losses will be considered which are classical in the literature on spherical flame balls, namely the 'near-field losses' and the 'far-field losses' models [6–8, 10]. The first model, where heat-losses are restricted to the burnt gas region, is known to be more appropriate for an asymptotic analysis and is therefore adopted in our analytical study. In our numerical study, on the other hand, both heat-loss models are addressed.

The paper is structured as follows. Section 2 provides the formulation of a constant density model describing axisymmetric flame balls in a two-dimensional mixing layer. The problem is shown to lead in the large-activation-energy asymptotic limit to a *free boundary problem* (FBP). The FBP is presented in Section 3 along with a summary of the corresponding analytical results in the adiabatic case including new formulas elucidating the effect of differential-diffusion. This is followed by the presentation of a new FBP

involving two dependent variables suitable for accounting for heat-loss from the burnt gas; the new FBP will be shown to lead to insightful formulas derived for weakly non-uniform mixtures. Numerical simulations, confirming and complementing the analytical findings and including a stability analysis, are presented in Section 4.

2. Formulation

The configuration for studying flame balls in a mixing layer is the same as the one adopted in [1, 2]. Namely, we consider a reactive mixture in a two-dimensional channel delimited by two porous plane walls located at $Z = \pm L$ as depicted in Figure 1, where useful notations are introduced. We note that this configuration is attractive in theoretical investigations [20–22] due to its simplicity, although it is difficult to achieve experimentally. Nevertheless, it is worth pointing out that successful experimental attempts to approximate it have been reported [23, 24].

Shown in the figure is an axisymmetric flame ball centred at a location $Z = Z_c$ (an eigenvalue) which is in general distinct from the location $Z = Z_{st}$ of the stoichiometric surface.

The combustion is represented by a one-step reaction of the form

$$\mathrm{F} + s\mathrm{O} \rightarrow (1+s)\mathrm{Product} + q,$$

where s and q denote the mass of oxidizer consumed and the heat released per unit mass of fuel. The reaction rate $\tilde{\omega}$, defined as the mass of fuel consumed per unit volume and unit time, is assumed to obey an Arrhenius law with pre-exponential factor B and activation energy E of the form

$$\tilde{\omega} = B\rho^2 Y_F Y_O \exp(-E/RT). \tag{1}$$

Here ρ, Y_F, Y_O, R and T represent the density, the fuel mass fraction, the oxidizer mass fraction, the universal gas constant, and the temperature, respectively.

For large activation energies, the region which is able to sustain significant heat generation is centred around the stoichiometric surface where $Y_O = sY_F$. In the frozen mixture far away from the flame ball, i.e. for $X^2 + Y^2 \rightarrow \infty$, the mass fractions profiles are linear

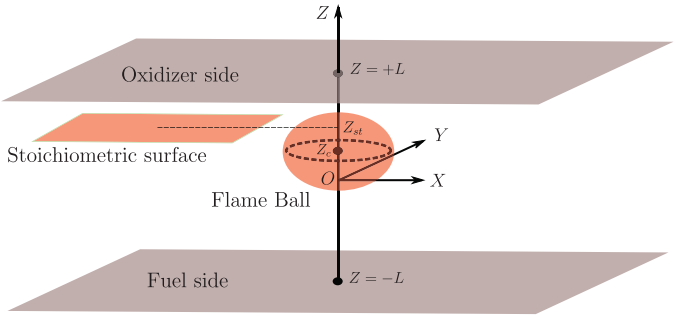

Figure 1. A flame ball in a non-uniform reactive mixture between two porous walls located a $Z = \pm L$. The mass fractions are prescribed by $Y_F = Y_{F,F}$ and $Y_O = 0$ on the fuel side, and $Y_F = 0$ and $Y_O = Y_{O,O}$ on the oxidizer side. The flame ball is centred at $Z = Z_c$ (an eigenvalue) which is in general distinct from the location $Z = Z_{st}$ of the stoichiometric surface.

functions of Z given by

$$Y_F = \frac{Y_{F,F}}{2}\left(1 - \frac{Z}{L}\right) \quad \text{and} \quad Y_O = \frac{Y_{O,O}}{2}\left(1 + \frac{Z}{L}\right),$$

and hence the stoichiometric surface is located at $Z = Z_{\rm st}$ with

$$\frac{Z_{\rm st}}{L} = \Delta \equiv \frac{S-1}{S+1}. \tag{2}$$

Here $S \equiv sY_{F,F}/Y_{O,O}$ is a normalised stoichiometric coefficient, known as the mixture equivalence ratio, and Δ a scaled version thereof which we shall use instead; the subscript 'st' will be used to indicate values at $(X^2 + Y^2 \to \infty, Z = Z_{\rm st})$ such as $Y_{F,{\rm st}} = Y_{F,F}(1-\Delta)/2$ and $Y_{O,{\rm st}} = Y_{O,O}(1+\Delta)/2$.

We now introduce the scaled quantities

$$y_F = \frac{Y_F}{Y_{F,F}}, \quad y_O = \frac{Y_O}{Y_{O,O}}, \quad \theta = \frac{T - T_u}{T_{ad} - T_u}.$$

Here,

$$T_{ad} \equiv T_u + \frac{qY_{F,F}}{2c_p}(1-\Delta),$$

where c_p is the mixture heat capacity, is the adiabatic flame temperature which is used to define the Zeldovich number $\beta \equiv E(T_{ad} - T_u)/RT_{ad}^2$ at the conditions prevailing at the stoichiometric location. At these conditions (and for $\beta \gg 1$), the laminar speed S_L of the stoichiometric planar flame with thickness $\delta_L \equiv D_T/S_L$, is given by

$$S_L = \sqrt{\frac{4{\rm Le_F Le_O}}{\beta^3} Y_{O,{\rm st}}(\rho D_T) B \exp(-E/RT_{ad})}, \tag{3}$$

where D_T, $\rm Le_F$ and $\rm Le_O$ are the thermal diffusivity, the fuel Lewis number and the oxidizer Lewis number, respectively.

The non-dimensional equations are given by

$$\frac{\beta}{\epsilon_L}\frac{\partial\theta}{\partial t} = \bar\nabla^2\theta + \frac{4}{1-\Delta^2}\frac{\beta^2}{\epsilon_L^2}(\omega - H(\theta)) \tag{4a}$$

$$\frac{\beta}{\epsilon_L}\frac{\partial y_F}{\partial t} = {\rm Le}_F^{-1}\bar\nabla^2 y_F - \frac{2}{1+\Delta}\frac{\beta^2}{\epsilon_L^2}\omega \tag{4b}$$

$$\frac{\beta}{\epsilon_L}\frac{\partial y_O}{\partial t} = {\rm Le}_O^{-1}\bar\nabla^2 y_O - \frac{2}{1-\Delta}\frac{\beta^2}{\epsilon_L^2}\omega, \tag{4c}$$

in terms of the coordinates

$$\bar x = \frac{X}{L}, \quad \bar y = \frac{Y}{L}, \quad \bar z = \frac{Z}{L}, \tag{5}$$

after selecting the mixing layer thickness L as unit length and L/S_L as a unit time and writing $\bar\nabla^2 = \partial_{\bar x\bar x} + \partial_{\bar y\bar y} + \partial_{\bar z\bar z}$. Note that the parameter ϵ_L represents the thickness of the planar stoichiometric flame measured with L/β; it is also related to the Damköhler number

Da defined as the ratio between the diffusion time across the mixing layer L^2/D_T and the flame time δ_L^2/D_T. Specifically, we have

$$\epsilon_L \equiv \frac{\delta_L}{L/\beta} = \frac{\beta D_T}{LS_L} \quad \text{and} \quad \text{Da} \equiv \frac{L^2}{\delta_L^2} = \beta^2 \epsilon_L^{-2}. \tag{6}$$

The non-dimensional reaction rate ω takes the form

$$\omega = \frac{\beta^3}{4\text{Le}_\text{F}\text{Le}_\text{O}} y_F y_O \exp\left(\frac{\beta(\theta-1)}{1+\alpha(\theta-1)}\right), \tag{7}$$

where $\alpha = (T_{ad} - T_u)/T_{ad}$.

The term $H(\theta)$ which appears in Equation (4a) is intended to account for heat-losses and can be set to zero in the adiabatic case where these are neglected. However, heat-losses are known to be important in flame ball studies, in particular as a stabilising mechanism when examining flame stability as discussed e.g. in references [6–8, 10, 25] where several models for $H(\theta)$ are considered [6–8, 10, 25]. Among these, we shall consider herein two simple models which we shall refer to as the 'near-field losses' and 'far-field losses' models following a terminology close to that of [6–8]. In the first model, $H(\theta)$ takes the form

$$H(\theta) = \frac{\kappa\theta}{\beta} \tag{8}$$

in the burnt gas and zero elsewhere, where κ will be referred to as the heat-loss coefficient. In the second model, this same form for $H(\theta)$ is adopted everywhere, both in the burnt and unburnt gases. We note that the 'near-field losses' model is known to conveniently lead to a consistent asymptotic solution in the asymptotic limit $\beta \to \infty$ (with $\kappa = O(1)$) in the classical case of spherical flame balls in an unbounded domain, for technical reasons discussed in [7], and hence it will be adopted to derive the asymptotic results to be presented below. In the numerical analysis undertaken, both models will be considered[1].

The boundary conditions corresponding to frozen profiles in the far field $\bar{x}^2 + \bar{y}^2 \to \infty$, and prescribed values on the walls $\bar{z} \to -1$ or $\bar{z} \to 1$, are

$$\theta = 0, \quad y_F = \frac{1-\bar{z}}{2}, \quad y_O = \frac{1+\bar{z}}{2}. \tag{9}$$

Equations (4) with the boundary conditions (9) complete the formulation of the problem (subject to suitable initial conditions). A main aim when tackling this problem is to find its stationary solutions (flame balls) and examine their stability. In particular, one would like to determine the domain of existence of these stationary solutions, and the corresponding profiles of θ, y_F, and y_O, in terms of the parameters ϵ_L, Δ, β, Le_F, Le_O and α. The analysis of these equations in the asymptotic limit $\beta \to \infty$ leads to a free boundary problem (FBP) presented in the next section along with its analytical solution for small values of ϵ_L. This is followed by a numerical investigation addressing the existence and stability of the flame balls.

3. Analytical results: the free boundary problem for flame balls in the limit $\beta \to \infty$

3.1. *The free boundary problem in the adiabatic case and its results*

In the limit $\beta \to \infty$, stationary solutions of Equations (4) with the boundary conditions (9), representing flame balls in the mixing layer, are solutions of a free boundary problem

(FBP). In the adiabatic case $H=0$, this FBP has been derived in [1] in the distinguished limit $\beta \to \infty$ with $\epsilon_L, l_F, l_O, x, y, z = \mathcal{O}(1)$. Here $l_F \equiv \beta(\mathrm{Le_F} - 1)$ and $l_O \equiv \beta(\mathrm{Le_O} - 1)$ are the reduced Lewis numbers and x, y and z non-dimensional coordinates[2] scaled by L/β defined by

$$x \equiv \frac{X}{L/\beta} = \beta\bar{x}, \quad y \equiv \frac{Y}{L/\beta} = \beta\bar{y}, \quad z = \frac{Z - Z_{st}}{L/\beta} = \beta(\bar{z} - \Delta), \tag{10}$$

where use has been made of (2) and (5).

The FBP consists of a single Laplace equation for the *leading order temperature* ψ to be solved outside a domain Ω (the burnt gas domain), with ψ required to vanish in the far field and to satisfy two conditions on the unknown boundary $\partial\Omega$ of Ω (the infinitely thin reaction sheet):

$$\nabla^2\psi = 0 \quad \text{in} \quad \mathbb{R}^3\backslash\Omega \tag{11a}$$

$$\psi = 0, \quad \text{as} \quad |\mathbf{r}| \to \infty \tag{11b}$$

$$\psi = 1, \quad \frac{\partial\psi}{\partial n} = -\epsilon_L^{-1}\mathcal{F} \quad \text{on} \quad \partial\Omega. \tag{11c}$$

Here $\mathcal{F}$ is an explicit function of $(z; \Delta, l_F, l_O)$ given by

$$\mathcal{F} = \sqrt{1 + \left|\frac{l_F - l_O}{2} + \frac{z}{1-\Delta^2}\right|}\, \exp\left\{\frac{-l_F - l_O}{4} - \frac{\Delta z}{2(1-\Delta^2)} - \left|\frac{l_F - l_O}{4} + \frac{z}{2(1-\Delta^2)}\right|\right\}. \tag{12}$$

For small values of ϵ_L, an analytical description of the solutions of the FBP (11) and the methodology to obtain them were presented in [1, 2] in the equidiffusional case $l_F = l_O$. Following the same methodology, new results pertaining to the more general case corresponding to arbitrary values of l_F and l_O can be derived. We shall simply record here a summary of these new results.

It is found that a flame ball can exist only if it is centred at a single location z_c of the symmetry axis, given to leading order as $\epsilon_L \to 0$ by

$$z_c \sim z_0 = -\Delta(1 + |\Delta|) + \frac{l_O - l_F}{2}(1 - \Delta^2). \tag{13}$$

In fact, z_0 is determined as an eigenvalue and it is found to correspond to the location of the maximum of the function $\mathcal{F}(z)$ given in (12). On account of (10), Equation (13) can also be written as

$$\bar{z}_c \equiv \frac{Z_c}{L} = \bar{z}_{st} + \frac{z_c}{\beta} \sim \Delta - \frac{1}{\beta}\left[\Delta(1 + |\Delta|) + \frac{l_O - l_F}{2}(1 - \Delta^2)\right], \tag{14}$$

which shows that the flame ball is centred at a location $\bar{z}_c$ which is distinct from the stoichiometric location $\bar{z}_{st} = \Delta$ except in the special case where the mixture is stoichiometrically balanced, $\Delta = 0$ (or $S = 1$) *and* equidiffusional, $l_F = l_O$. Although the difference

between $\bar{z}_c$ and $\bar{z}_{st}$ is small, of order β^{-1}, it is significant. Indeed, this difference leads to an $O(1)$ difference in the size of the flame balls in a uniform mixture at the conditions prevailing at $\bar{z}_c$ and $\bar{z}_{st}$ and hence has a significant impact when estimating the minimum critical energy for ignition based on these two locations (see Equation (19) below).

Using the expression of z_0 in (13), we define a small expansion parameter ϵ, a rescaled version of ϵ_L, by

$$\epsilon = \frac{\epsilon_L}{\mathcal{F}_0} \quad \text{where } \mathcal{F}_0 \equiv \mathcal{F}(z_0) = \frac{\mathrm{e}^{-|\Delta|/2}}{(1-|\Delta|)^{1/2}} \mathrm{e}^{-(l_F+l_O)/4-(l_O-l_F)\Delta/4}, \tag{15}$$

and carry a perturbation analysis for small values of ϵ. This leads to the following expansions

$$\psi = \frac{1}{r} + \frac{b\epsilon^2}{3}\left(\frac{1}{r} + \frac{1}{r^3} - \frac{3\cos^2\theta}{r^3}\right) \tag{16}$$

$$R = 1 + \frac{b\epsilon^2}{3}\left(2 - 3\cos^2\theta\right) \tag{17}$$

$$V = \frac{4\pi}{3}\left(1 + b\epsilon^2\right) \tag{18}$$

$$\frac{E_B}{E_Z} = \frac{\mathcal{F}_{st}^3}{\mathcal{F}_0^3}\left(1 + b\epsilon^2\right), \tag{19}$$

where

$$b = \frac{1}{4\,(1+|\Delta|)^2}, \tag{20}$$

and

$$\mathcal{F}_{st} \equiv \mathcal{F}(z=0) = \sqrt{1 + \left|\frac{l_F - l_O}{2}\right|} \exp\left\{\frac{-l_F - l_O}{4} - \left|\frac{l_F - l_O}{4}\right|\right\}. \tag{21}$$

These expressions are obtained after rewriting the problem in terms of spherical coordinates centred at $(x, y, z) = (0, 0, z_c)$ and rescaled such that

$$(x, y, z - z_c) = \epsilon(r\sin\theta\cos\phi, r\sin\theta\sin\phi, r\cos\theta). \tag{22}$$

The expansions describe axisymmetric solutions where $r = R(\theta)$ represents the domain boundary $\partial\Omega$ and ψ the temperature field for $r > R(\theta)$, i.e. outside the burnt gas region. The rescaled coordinate r corresponds to choosing as unit length $\delta_L/\mathcal{F}_0$, which is the radius of the spherical Zeldovich flame ball at the conditions prevailing at z_0 as confirmed by the limit $R \to 1$ as $\epsilon \to 0$ implied by (17). On account of (6) and (15), ϵ is seen to represent a non-dimensional measure of this spherical flame ball radius based on the length L/β.

The non-dimensional volume V of the distorted flame ball, given by

$$V \equiv 2\pi \int_0^{\pi} \int_0^{R(\theta)} r^2 \sin\theta \, \mathrm{d}r \, \mathrm{d}\theta, \tag{23}$$

is evaluated using the expression (17) for $R(\theta)$ which yields formula (18) after expanding to $O(\epsilon^2)$. The corresponding dimensional volume of the distorted flame ball is $V_B = V\delta_L^3/\mathcal{F}_0^3$. On the other hand, the dimensional volume of the spherical Zeldovich flame ball at the

conditions prevailing at the stoichiometric location $z=0$ is given by $V_Z = (4\pi/3)\delta_L^3/\mathcal{F}_s^3$, given that $\delta_L/\mathcal{F}_s$ is the radius of the latter. The thermal energies inside V_B and V_Z are denoted by E_B and E_Z, respectively. These are given by $E_B = \rho c_p(T_{ad} - T_u)V_B$ and $E_Z = \rho c_p(T_{ad} - T_u)V_Z$ where c_p is the heat capacity, when non-dimensional temperature variations of order β^{-1} are neglected, and hence their ratio is given by (19). Equation (19) shows that $E_B > E_Z$, since $\mathcal{F}_0$ is the maximum of the function $\mathcal{F}(z)$ (which occurs at $z = z_0$). This indicates that it is more difficult to ignite the mixture if external energy is deposited at the stoichiometric location ($z=0$) rather than at the optimum location $z = z_0$. Of course, the analytical formulas (14) and (19) allow a better appreciation of this statement given the simple explicit dependence on the parameters which they exhibit.

3.2. *The free-boundary problem with heat-loss*

In the asymptotic results presented above we have discarded heat-loss effects. These are known however to be important in many circumstances, in particular when the concentration of the reactants is weak. They are also important as a stabilising factor in any stability analysis, as undertaken in the next section. Here, we present a generalisation of the free-boundary problem of the previous section to account for heat-losses. To this end, we again consider the asymptotic limit $\beta \to \infty$ and consider 'near-field heat losses' such that the heat-loss term $H(\theta)$ in (4a) is of the form $\kappa\theta/\beta$ in the burnt gas and zero elsewhere; as noted in the paragraph following Equation (7) this form is known to lead to a consistent asymptotic solution in the classical spherical case[3]. The free-boundary problem is found to generalise to

$$\nabla^2\psi = 0, \quad \nabla^2\phi = 0 \quad \text{in} \quad R^3\backslash\Omega \tag{24a}$$

$$\psi = 1, \quad \nabla^2\phi = \epsilon_L^{-2}\kappa \quad \text{in} \quad \Omega \tag{24b}$$

$$\psi = 0, \quad \phi = 0 \quad \text{as} \quad |\mathbf{r}| \to \infty \tag{24c}$$

$$[\psi] = [\phi] = [\phi_n] = 0, \quad [\psi_n] = -\mathrm{e}^{\phi/2}\epsilon_L^{-1}\mathcal{F} \quad \text{on} \quad \partial\Omega. \tag{24d}$$

Here, $\psi \equiv \theta^0$ is again the leading order temperature when expansions in terms of $1/\beta$ of the form $\theta \sim \theta^0 + \theta^1/\beta$, $y_F \sim y_F^0 + y_F^1/\beta$ and $y_O \sim y_O^0 + y_O^1/\beta$ are used. The quantity ϕ is defined by $\phi = l_F\theta^0 + \theta^1 + 2y_F^1/(1-\Delta) + z/(1-\Delta)$ and $\phi = l_O\theta^0 + \theta^1 + 2y_O^1/(1+\Delta) - z/(1+\Delta)$; this double definition of ϕ is permissible as the functions given by the right hand sides in the two definitions can be shown to satisfy the same equation and auxiliary conditions, those given for ϕ. The justification of this statement and the derivation of the free boundary value problem (24) follow from applying an asymptotic methodology similar to that of [1, 26, 27], which begins by introducing the expansions in terms of $1/\beta$ just mentioned in the governing equations and using the distinguished limit $\beta \to \infty$ with ϵ_L, l_F, l_O, κ, x, y, $z = \mathcal{O}(1)$. We shall skip the rather lengthy but straightforward algebraic details, and restrict ourselves to presenting the main analytical result corresponding to the free boundary problem (24) derived for small values of ϵ_L.

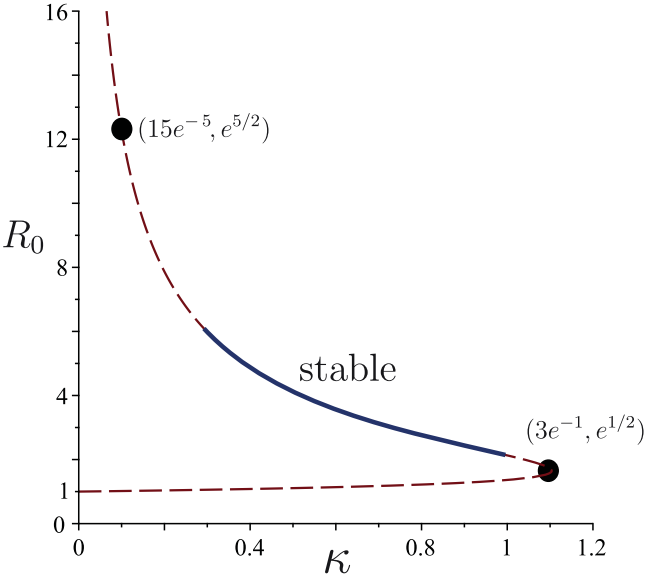

Figure 2. Flame ball radius R_0 versus κ. The solid line represents stable solutions which exist only if the effective Lewis number is sufficiently below one. The lower dot pertains to the turning point at $(\kappa, R_0) = (3\,\mathrm{e}^{-1}, \mathrm{e}^{1/2})$ to the right of which there are no stationary solutions. The upper dot pertains to the point at $(\kappa, R_0) = (15\,\mathrm{e}^{-5}, \mathrm{e}^{5/2})$ above which all stationary solutions are unstable to 3D disturbances.

To leading order, as $\epsilon_L \to 0$, we find that the flame ball is spherical with radius R_0 such that

$$R_0 = \mathrm{e}^{\kappa R_0^2/6}. \tag{25}$$

This is the same result as the one found in the literature on flame balls in uniform mixtures, see e.g. [6–8]. A plot of R_0 versus κ is shown in figure 2 and indicates that two branches of solutions exist for κ less than a critical value $\kappa_{\mathrm{crit}} = 3\,\mathrm{e}^{-1}$. Solutions on the lower branch (corresponding to smaller flame balls) are known to be unstable, while the upper branch possesses a stable portion (indicated by a solid line) if the Lewis number of the deficient reactant is below a critical value which is strictly less than one [8]. As the Lewis number is decreased towards zero, the stable portion extends to cover the whole upper branch according to a linear analysis of stability to one-dimensional disturbances; linear analysis of stability to three-dimensional disturbances shows however that stable solutions cannot exist for $R_0 > \mathrm{e}^{5/2}$, irrespective of the value of the Lewis number [8]. Therefore, stable flame balls cannot be neither too large nor too small, and must satisfy the necessary (but not sufficient) condition $\mathrm{e}^{1/2} < R_0 < \mathrm{e}^{5/2}$. One aim of this paper is to examine, as done below numerically, how these conclusions pertaining to the stability of flame balls in a uniform mixture are affected by the mixture non-uniformity included in our model.

To next order we find that

$$R = R_0 + b\epsilon^2 R_0^3 \left(\frac{1}{3 - \kappa R_0^2} + \frac{5}{15 - \kappa R_0^2}(1 - 3\cos^2\theta) \right), \tag{26}$$

where b is as in (20) and ϵ is given by (15).

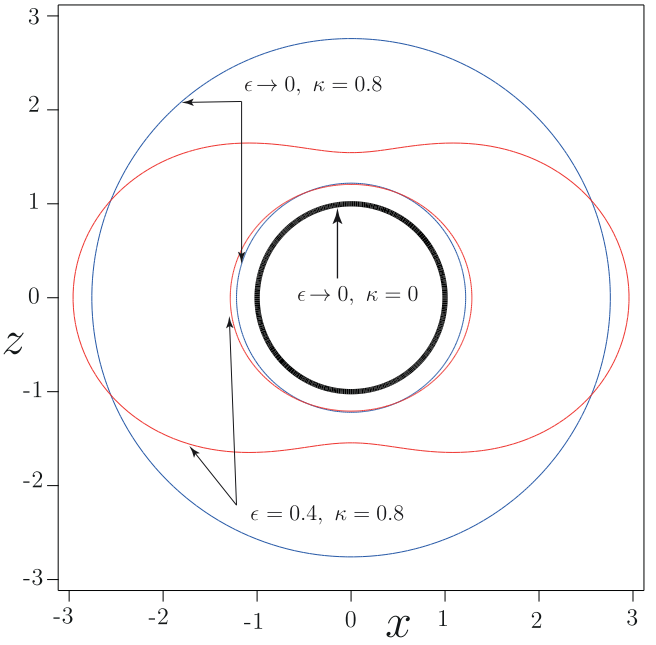

Figure 3. Flame ball shape $R(\theta)$ plotted in the xz plane for selected values of ϵ and κ based on Equation (26). Three cases are shown: uniform adiabatic case ($\epsilon = 0, \kappa = 0$) (one spherical ball), uniform nonadiabatic case ($\epsilon = 0, \kappa = 0.8$) (two spherical balls) and non-uniform non-adiabatic case ($\epsilon = 0.4, \kappa = 0.8$) (two non-spherical balls).

The equation describes how the non-uniformity of the mixture distorts the spherical flame balls. This is shown graphically in Figure 3 which illustrates the combined effect of ϵ and κ on the flame shape.

The volume V of the distorted flame ball, given by (23), can de evaluated using the expression for $R(\theta)$ given in (26), which yields after expanding to $O(\epsilon^2)$

$$V = \frac{4\pi R_0^3}{3}\left(1 + \frac{3bR_0^2}{3 - \kappa R_0^2}\epsilon^2\right).$$

The leading order is of course the volume corresponding to the spherical flame ball with radius $R_0 = R_0(\kappa)$ given in (25). It is convenient to define the *equivalent radius* R_{eq} as being the radius of a sphere having the same volume V, that is $V = 4\pi R_{\text{eq}}^3/3$. To $O(\epsilon^2)$, we thus have

$$R_{\text{eq}} = R_0 + \frac{bR_0^3}{3 - \kappa R_0^2}\epsilon^2. \tag{27}$$

For selected values of ϵ, plots of R_{eq} versus κ, similar to the plot of Figure 2, should provide a meaningful global assessment of the effect of non-uniformity measured by ϵ. However, if expansion (27) is used as it is to this end, erroneous results will be obtained in the vicinity of the turning point of the leading order $R_0(\kappa)$, that is for $\kappa \to 3\,\mathrm{e}^{-1}$ or equivalently $R_0 \to \mathrm{e}^{1/2}$, as the second term in the expansion becomes clearly more singular than the first in this limit. This is not surprising as such non-uniformity in expansions where the leading order term has a singularity are common, and can be remedied in principle

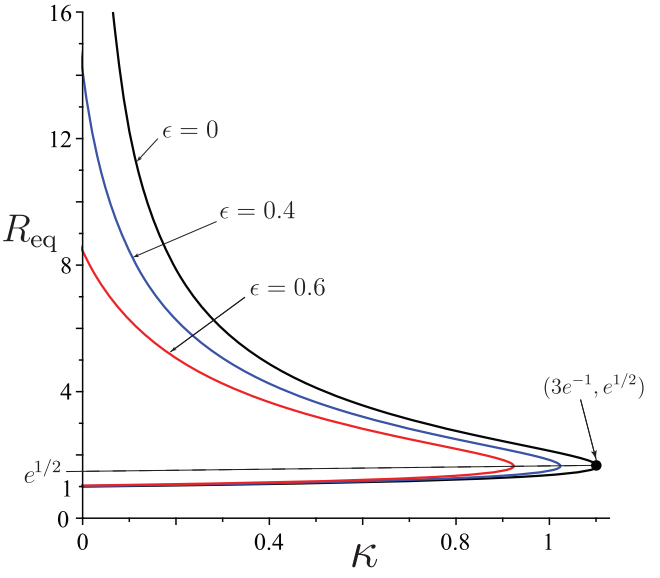

Figure 4. The flame ball equivalent radius $R_{\rm eq}$ versus κ for selected values of ϵ and $b = 1/4$.

by the method of renormalisation [28, 29]. The method consists roughly in expanding the relevant independent variable itself in such a way so as to render each term in the expansion of the dependent variable less singular than the term of lower order. Although applicable in our case, we shall not use this method as a more straightforward remedy is to notice that expansion (27) can be rewritten in the form

$$R_{\rm eq} = R_0(\kappa + 2b\epsilon^2), \tag{28}$$

where the parentheses on the right hand side contain the argument of the (bi-valued) function $R_0(\kappa)$. Indeed, (27) can be recognised as a Taylor expansion valid to $O(\epsilon^2)$ of Equation (28) on account of the definition of R_0 in (25). Formula (28) provides an elegant and simple interpretation of the effect of ϵ (and in fact of all the parameters entering in the definition of ϵ and b given by (15) and (20)) on the equivalent radius $R_{\rm eq}$. Specifically, the curve of $R_{\rm eq}$ versus κ is the same as the curve of $R_0(\kappa)$ shifted to the left by $2b\epsilon^2$. This result has significant implications regarding the existence and the size of the flame balls, as illustrated in Figure 4 where $R_{\rm eq}(\kappa)$ is plotted for selected values of ϵ and $b = 1/4$ (a stoichiometrically balanced mixture with $\Delta = 0$). For example, for any $\epsilon > 0$, it is clear that flame balls can exist only if $\kappa < 3\,{\rm e}^{-1} - 2b\epsilon^2$ and their equivalent radius $R_{\rm eq}$ cannot be arbitrary large (as in the case $\epsilon = 0$, disregarding stability aspects) but has a finite maximum value which decreases with ϵ.

Before closing this section, we simply mention that the non-uniformity in the expansion (27) for $R_{\rm eq}$ can be traced to the non-uniformity in the expansion (26) for R. The second term of (26) contains the singularity associated with the turning point of the leading order $R_0(\kappa)$ corresponding to $\kappa \to 3\,{\rm e}^{-1}$ or equivalently $R_0 \to {\rm e}^{1/2}$ and also an additional singularity corresponding to $\kappa \to 15\,{\rm e}^{-5}$ or equivalently $R_0 \to {\rm e}^{5/2}$. It is interesting to note that this additional singularity corresponds to the point, shown in Figure 2, and identified in [6, 8] in the analysis of stability of flame balls to 3D perturbations. As done above to write the more meaningful expression (28) for $R_{\rm eq}$, a similar more meaningful expression

may be written for R as

$$R = R_0\left(\kappa + \epsilon^2 f(\kappa,\theta)\right), \tag{29}$$

where the outer parentheses on the right hand side contain the argument of the function $R_0(\kappa)$ and where the function f is given by

$$f(\kappa,\theta) = 2b\left[1 + \frac{1 - 2\ln R_0(\kappa)}{1 - \frac{2}{5}\ln R_0(\kappa)}\left(1 - 3\cos^2\theta\right)\right].$$

Indeed, (26) can be recognised as a Taylor expansion valid to $O(\epsilon^2)$ of Equation (29) on account of the definition of R_0 in (25).

4. Numerical Results including a stability analysis

In this section we present illustrative numerical results of the finite-β problem of Section 2. We also examine the stability of the axisymmetric flame balls, and identify cases where they are indeed stable.

The numerical solutions to the problem given by Equations (4) subject to boundary conditions (9) and suitable initial conditions are obtained using the method described in [2, 21, 22, 30] which we have tested extensively in several combustion applications. Briefly, the set of equations are solved using the finite-element package Comsol Multiphysics on a non-uniform grid of triangular elements, with particular refinement around the reaction zone. The results are tested to ensure that they are not dependent on the mesh. All calculations are performed for $\beta = 10$, $\alpha = 0.85$, $\Delta = 0$ and $\mathrm{Le_O} = 1$, unless otherwise stated.

4.1. *Effect of the Lewis number on the flame ball (adiabatic case)*

We begin by describing the effect of varying the fuel Lewis number $\mathrm{Le_F}$ on the flame ball in the adiabatic case $H \equiv 0$; for simplicity $\mathrm{Le_O}$ is kept fixed equal to one throughout. Figure 5 illustrates how the flame ball shape and location are affected by variations in $l_F \equiv \beta(\mathrm{Le_F} - 1)$. Plotted is the flame ball shape, represented numerically by the temperature iso-contour $\theta = \theta_{\max}(1 - 2\beta^{-1})$, for selected values of ϵ_L and l_F. It's seen that an increase of l_F for a fixed value of ϵ_L shifts the flame ball centre downwards towards the fuel side and increases the flame ball size. Conversely, a decrease in l_F shifts the flame ball upwards towards the oxidizer side and decreases its size. These observations are in agreement with the asymptotic formulas (14), (15), and (18) of Section 3.1, at least for small values of ϵ_L.

Another important effect of the Lewis number is associated with its influence on the existence domain of the flame ball. In the adiabatic case, this existence domain, determined numerically, corresponds to the shaded region in the l_F-ϵ_L plane which is below and to the left of the lower curve plotted in Figure 6. It is seen that an increase/decrease in l_F decreases/increases the ϵ_L-range where flame balls exist. In this figure, we have also plotted the extinction curve of the planar diffusion flame in our configuration; the diffusion flame existence domain is to the left of this upper curve and is seen to include the flame ball existence domain. Therefore, under adiabatic conditions, flame balls may only exist under conditions which permit the existence of diffusion flames. This conclusion becomes invalid when heat-losses are taken into account, as in the cases described by the next three figures which address the combined influence of heat-loss and preferential diffusion.

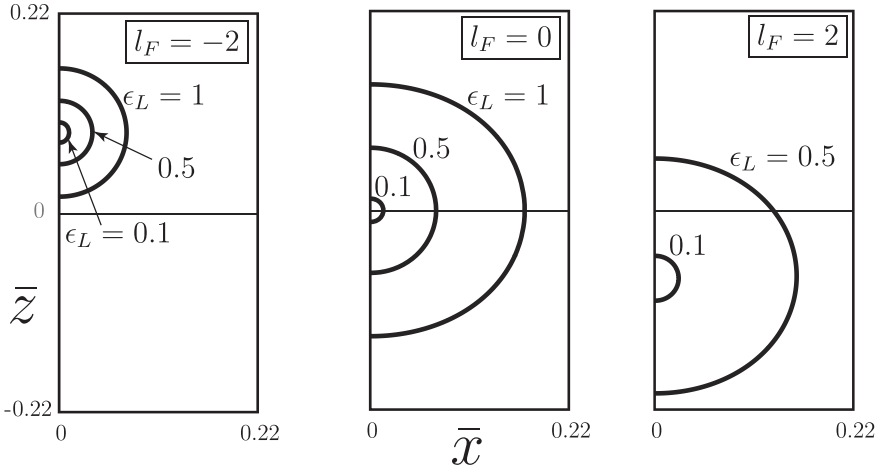

Figure 5. Plots in the $\bar{x}$-$\bar{z}$ plane of the flame shape, defined numerically by $\theta = \theta_{\max}(1 - 2\beta^{-1})$, for selected values of ϵ_L and $l_F = -2$ (left subfigure), $l_F = 0$ (middle subfigure) and $l_F = 2$ (right subfigure).

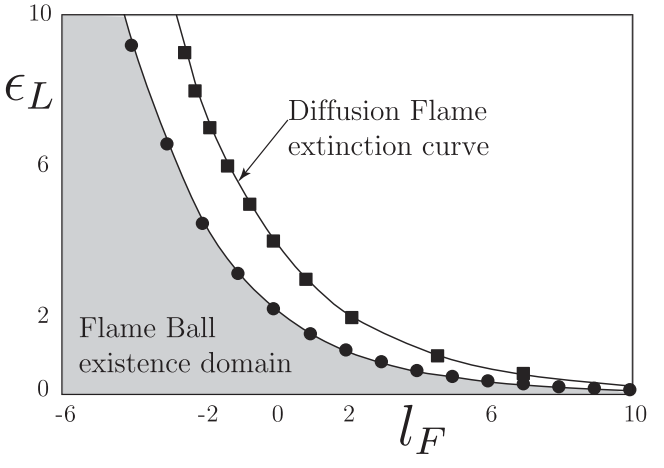

Figure 6. Existence domain of the flame ball in the l_F-ϵ_L plane in the *adiabatic case* (shaded area). Also plotted is the extinction curve of the planar diffusion flame.

4.2. *Combined influence of heat-loss and preferential diffusion on the existence domain*

In this section, we shall adopt the 'far-field heat losses' model introduced above, that is with the heat-loss term being given by (8) in the whole domain. In the next section, 'near-field heat losses' are also considered.

Figure 7 illustrates how the flame ball existence domain in the l_F-ϵ_L plane is influenced by the heat-loss parameter κ. Plotted are curves representing the boundary of this domain, to the left of which flame balls exist, for selected values of κ. A straightforward observation is that the existence domain shrinks with increasing values of κ, in conformity with our expectation. More importantly, we note that a turning point in the domain boundary is

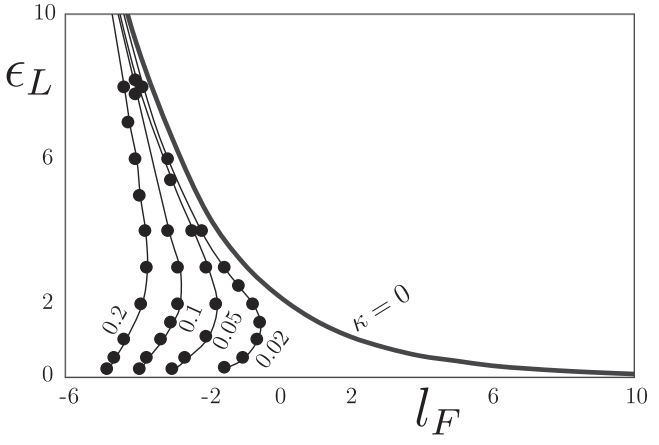

Figure 7. Existence domain of the flame ball in the $l_F - \epsilon_L$ plane for selected values of the heat-loss parameter κ. For a given value of κ, the flame ball exists to the left of the curve labelled with this value.

present for any $\kappa > 0$, while none is found for $\kappa = 0$. For a given $\kappa > 0$, we shall denote by (l_F^*, ϵ_L^*) the turning point of the domain boundary where a lower branch, say $\epsilon_L^{min}(l_F)$, and an upper branch, say $\epsilon_L^{max}(l_F)$, merge. The presence of the turning point has several physically meaningful consequences. It implies, for example, that the flame ball may exist only if l_F is bounded above, namely for $l_F < l_F^*$, while no such upper bound occurs when $\kappa = 0$. It implies also that a necessary condition for the flame ball existence, not too far from the turning point, is that ϵ_L must be in the finite range $[\epsilon_L^{min}, \epsilon_L^{max}]$, where $\epsilon_L^{min} > 0$ as seen from the figure. This means that, as ϵ_L is varied, flame balls fail to exist either when they become too large or too small. Furthermore, the strict inequality $\epsilon_L^{min} > 0$ demonstrate the occurrence of cases pertaining to specific values of κ and l_F for which non-spherical flame balls (corresponding to $\epsilon_L > 0$) exist but spherical flame balls in the uniform mixture at the stoichiometric conditions (obtained in the limit $\epsilon_L \to 0$) cannot exist. In other words, the non-uniformity of the mixture, whose strength vanishes in the limit $\epsilon_L \to 0$, is necessary in these cases for the existence of the flame ball.

It is worth noting that the occurrence of the turning point in the boundary of the flame ball existence domain is also found in the extinction curve of the diffusion flame when $\kappa > 0$. This is illustrated in Figure 8 where the diffusion flame extinction curve and the flame ball existence domain are displayed for $\kappa = 0.02$; also plotted for sake of reference the diffusion flame extinction curve for $\kappa = 0$. We note that the diffusion flame extinction curve is an inverse-C shaped curve when $\kappa > 0$. The points on the upper branch represent extinction at small values of the Damköhler number (large ϵ_L) due to the phenomenon of 'flame quenching' (triggered by a fast supply of reactants to the reaction zone) which is also operative in the adiabatic case $\kappa = 0$. The points on the lower branch represent extinction at large values of the Damköhler number (small ϵ_L) due to heat-loss; this type of extinction with fast chemistry is mainly associated with the fact that the rate of heat generation by the chemical reaction decreases as ϵ_L (or the rate of reactant supply to the reaction zone) is decreased, leading to extinction for any non-zero value of κ. Both types of extinction are known in the literature on diffusion flames in similar configurations [31–35].

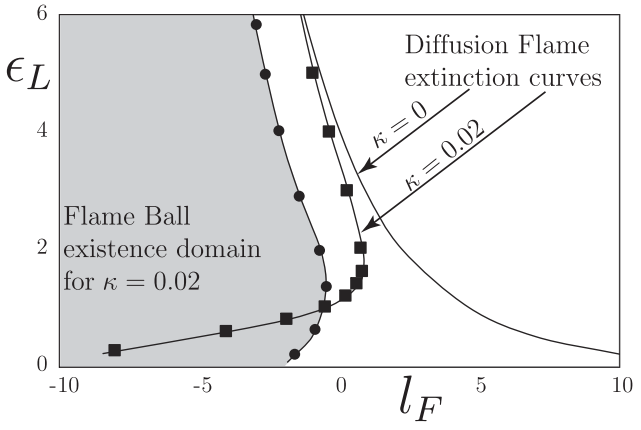

Figure 8. Flame ball existence domain for $\kappa = 0.02$ in the $l_F - \epsilon_L$ plane along with the diffusion flame extinction curves for $\kappa = 0.02$ and $\kappa = 0$.

Another informative way to characterise the existence domains of the flame ball and of the diffusion flame is to delimit these domains in the κ-ϵ plane for fixed values of l_F. For $l_F = -2$ this is done in Figure 9. We note that four regions can be identified which are labelled by roman numerals. In region I both the flame ball and the diffusion flame can exist, in region II only the flame ball exists but not the diffusion flame, in region III only the diffusion flame exists, and in region IV none of these solutions may exist. We note that the

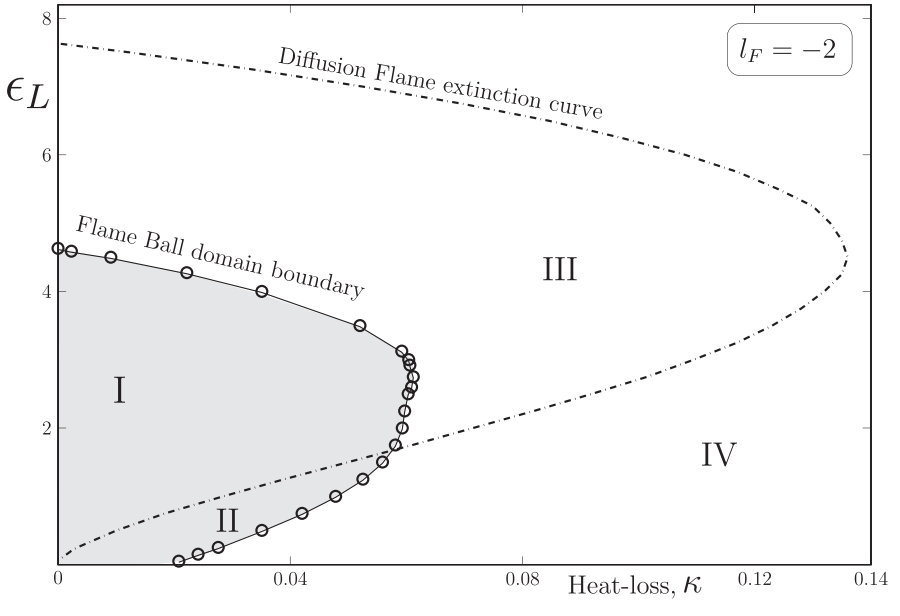

Figure 9. Flame ball existence domain (delimited by solid line) and diffusion flame extinction curve (dashed line) for $l_F = -2$. Four regions labelled by roman numerals are identified. In region I both the flame ball and the diffusion flame can exist, in region II only the flame ball exists but not the diffusion flame, in region III only the diffusion flame exists, and in region IV none of these solutions may exist.

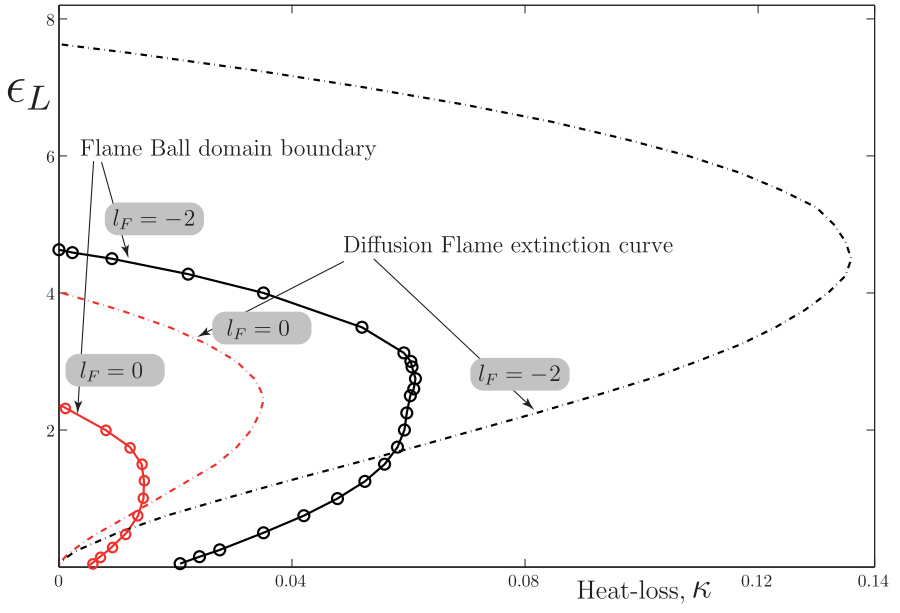

Figure 10. Existence domains of Flame Balls (delimited by solid line) and Diffusion Flame (delimited by dashed line) for two selected values of l_F.

subdivision of the κ-ϵ plane into such four regions remains valid for zero and moderately large positive values of l_F, with the main effect of increasing l_F being to shrink the size of the regions I, II, and III where flame ball and/or the diffusion flame can exist. This can be seen in Figure 10 where the boundaries of these domains are plotted for $l_F = 0$ and $l_F = -2$. We note that the subdivision of the κ-ϵ plane aforementioned provides useful insight regarding the possible modes of burning, ignition, and extinction in the mixing layer. For example, since in region III flame ball cannot exist, any Zeldovich type ignition theory based on flame balls cannot be extended to diffusion flames in this region, that is for sufficiently large values of κ and ϵ_L. Another interesting result is that the flame balls may exist in situations where the diffusion flame cannot. This occurs for conditions pertaining to region II in Figure 9 which are able to sustain burning in the form of flame balls but not in the form of planar diffusion flames. The variety of shapes the flame ball solutions take in regions I and II is illustrated in Figures 11 and 12 pertaining to $\epsilon = 0.5$ and $\epsilon = 2$, respectively, and to several selected values of κ. A particularly interesting type of solutions identified corresponds to ring-shaped structures seen e.g. in case (e) of Figure 11. These non-propagating solutions, which may be termed 'flame rings', are found in parts of region II due to local extinction near the vertical symmetry axis. The extinction occurs for elongated flame balls for which the conditions near the axis are such that the flame there may be approximated as a portion of a planar diffusion flame which cannot exist.

4.3. *Stability of the flame balls*

The existence of flame balls as stationary solutions of the governing equations considered in the previous section is an essential step preceding a stability analysis of these structures which we now address. We note beforehand that both the existence of the flame balls and

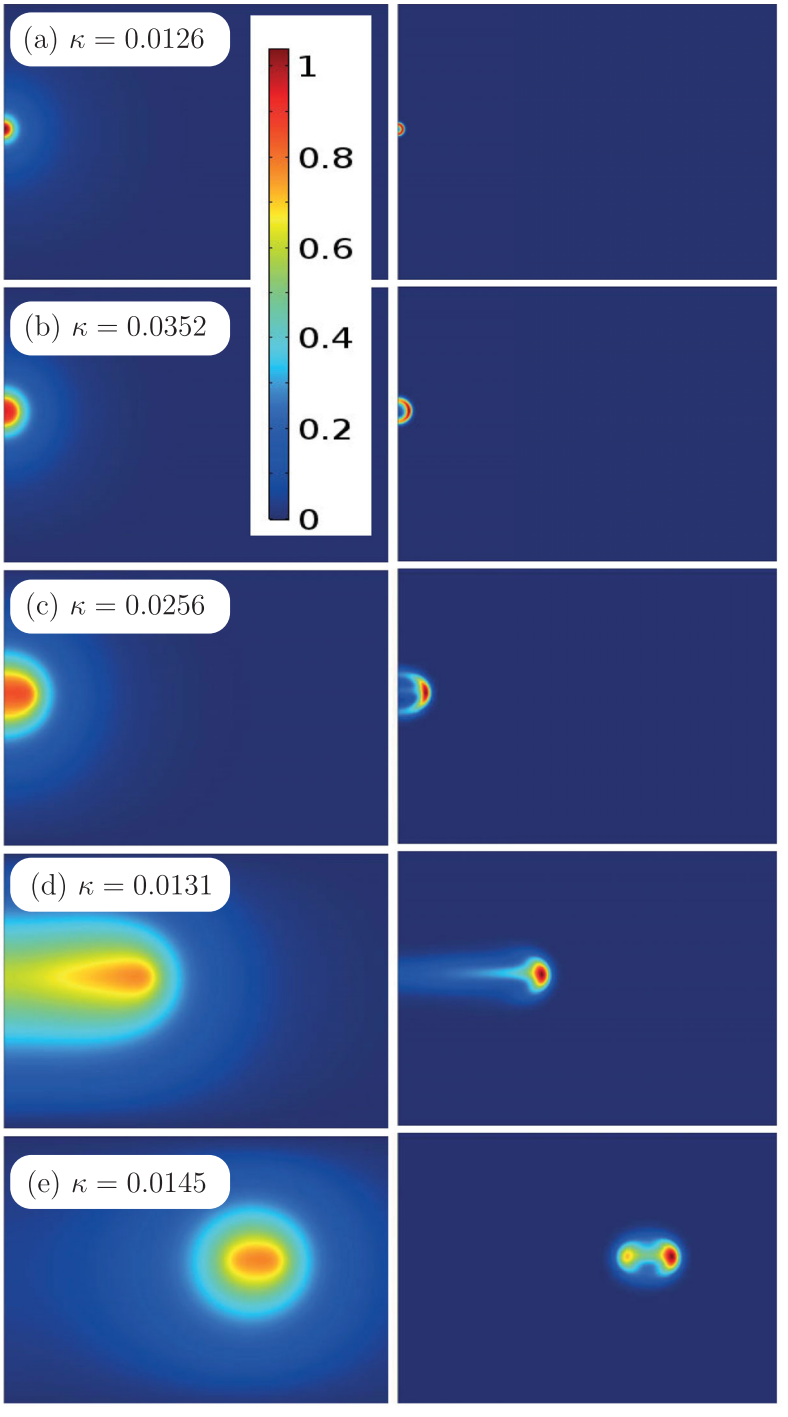

Figure 11. Temperature θ (left) and reaction rate ω (right) for $l_F = -2$, $\epsilon_L = 0.5$ and selected values of κ. The colour bar indicates the common temperature scale for all left subfigures; the w-field in each of the right subfigures has its own colour-scale (for sake of clarity). The figures are cross sections in the $\bar{x}$-$\bar{z}$ plane, with the range of the horizontal $\bar{x}$-axis displayed being $[0, 2.75]$, and that of the vertical $\bar{z}$-axis being $[-1, 1]$.

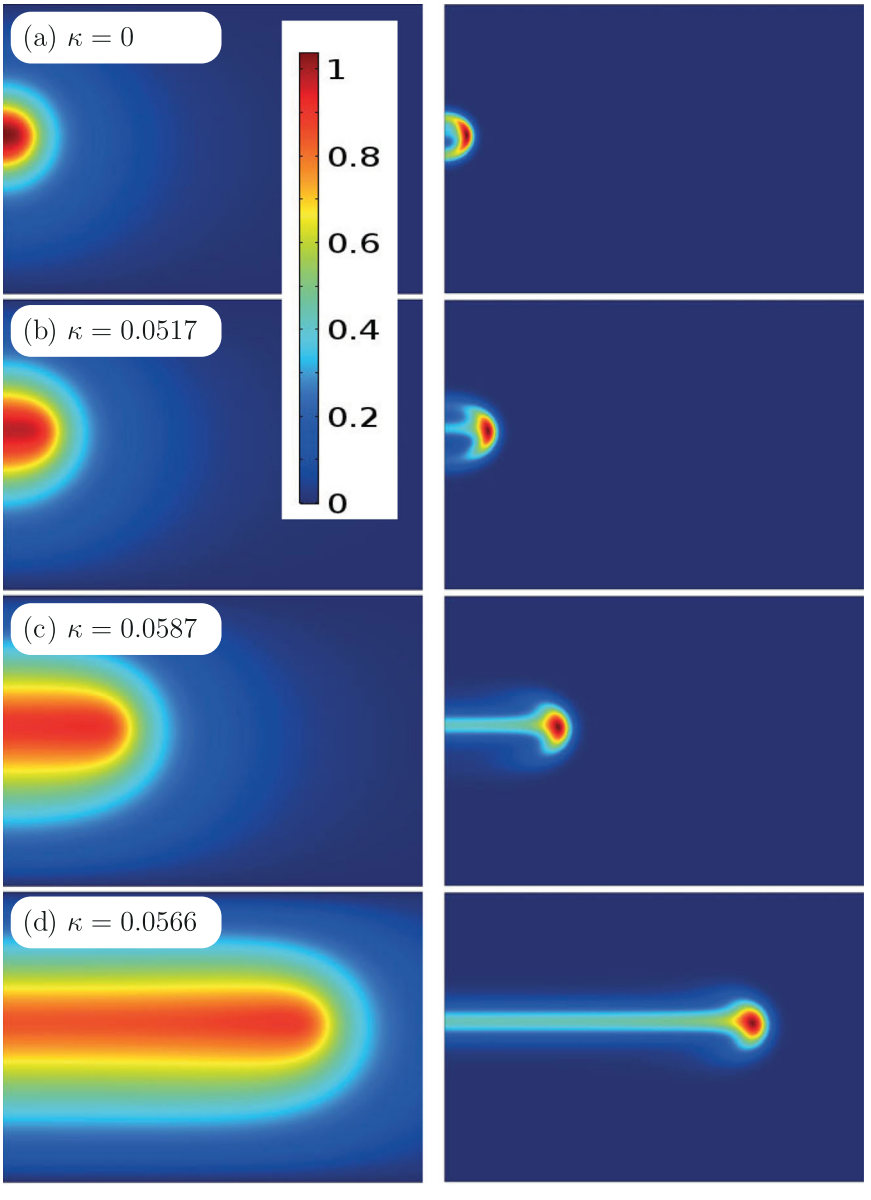

Figure 12. Temperature θ (left) and reaction rate ω (right) for $l_F = -2$, $\epsilon_L = 2$ and selected values of κ. The colour bar indicates the common temperature scale for all left subfigures. The figures are cross sections in the $\bar{x}$-$\bar{z}$ plane, with the range of the horizontal $\bar{x}$-axis displayed being $[0, 2.75]$, and that of the vertical $\bar{z}$-axis being $[-1, 1]$.

their stability are expected to be sensitive to the heat-loss model adopted, as suggested by studies related to the spherical flame balls in uniform mixtures [6–8]. We shall confirm that these suggestions remain valid in our non-uniform case. For example, adoption of the 'near-field losses model', where κ in Equation (8) is set to zero outside the burnt gas, leads to an existence domain shown in Figure 13 which presents quantitative and qualitative

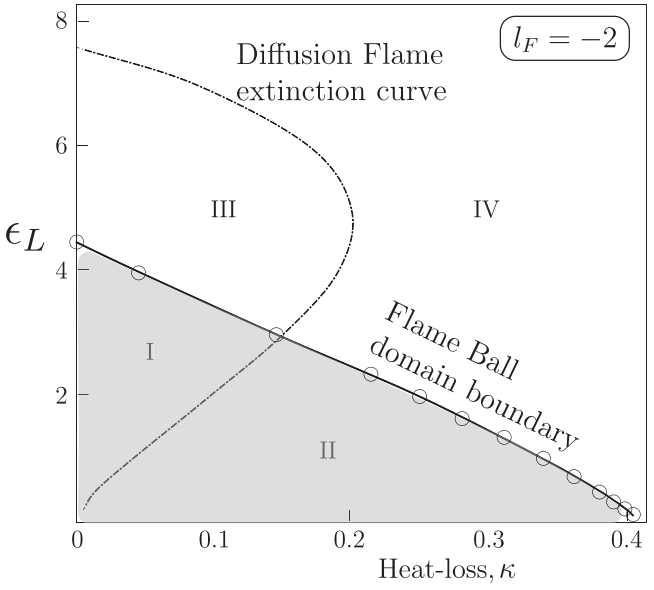

Figure 13. Flame ball existence domain (delimited by solid line) and Diffusion Flame extinction curve (dashed line) for $l_F = -2$ for the 'near-field losses model'. As in Figure 9, four regions labelled by roman numerals are identified. In region I both the flame ball and the diffusion flame can exist, in region II only the flame ball exists but not the diffusion flame, in region III only the diffusion flame exists, and in region IV none of these solutions may exist.

differences with the existence domain corresponding to the 'far-field losses model' shown in Figure 9. Without repeating the discussion of the previous section, we simply note the existence in both figures of the four regions introduced above, with a notable qualitative change in the flame ball domain boundary which is now monotonically decreasing with κ.

We summarise now the results pertaining to the stability of the flame balls. The stability of a given stationary solution is determined numerically by solving the unsteady governing equations with initial condition corresponding to the stationary solution modified by the addition of small random perturbations of small amplitude (of the order of 10^{-4}) which are localised in a region several times the size of the flame ball.

Consider first the stability of the flame balls within the 'near-field losses model' which was adopted in the analytical investigation of Section 3.2. For unit Lewis numbers, we have found that all flame balls are unstable, as expected. The question arises whether stable flame balls do exist in our non-uniform mixture. Figure 14 exhibits a case, corresponding to $l_F = -2$ and $\epsilon_L = 0.5$, where such stable solutions (solid line on the upper branch) do exist; the subfigure shows how a perturbed solution on the lower branch (corresponding to an unstable small flame ball) evolves towards a stable larger flame ball on the upper branch. We note that our conclusions are similar to those found in investigations on spherical flame balls in uniform mixtures with a 'near-field heat losses model' [6, 8], as discussed in connection with Figure 2. Figure 15 shows a similar situation with a larger value of ϵ_L, where the whole upper branch is found to consist of stable solutions.

Next, we address the stability of the flame balls within the 'far-field losses model'. Illustrative results are presented in Figures 16 and 17. In particular, these figures show that no stable solutions exist now (with far-field heat-losses allowed) for $\epsilon_L = 0.5$ while such

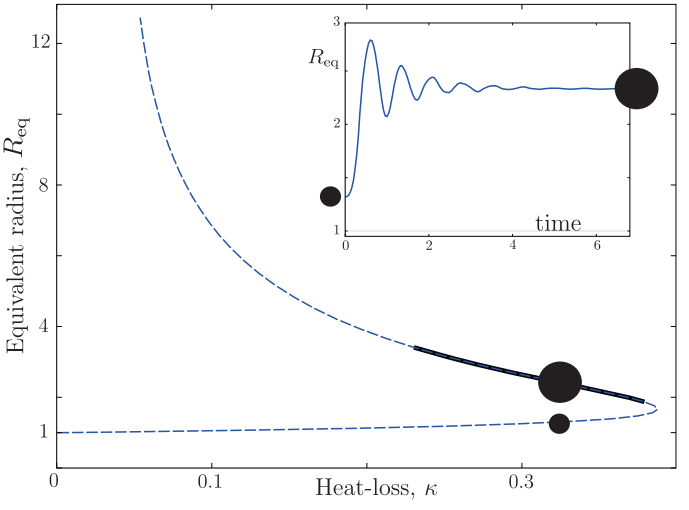

Figure 14. Flame Ball equivalent radius R_{eq} versus heat-loss parameter κ for $l_F = -2$ and $\epsilon_L = 0.5$. Solid line represents stable solutions. Subfigure: an unstable FB evolving to a larger stable FB ($\kappa = 0.33$).

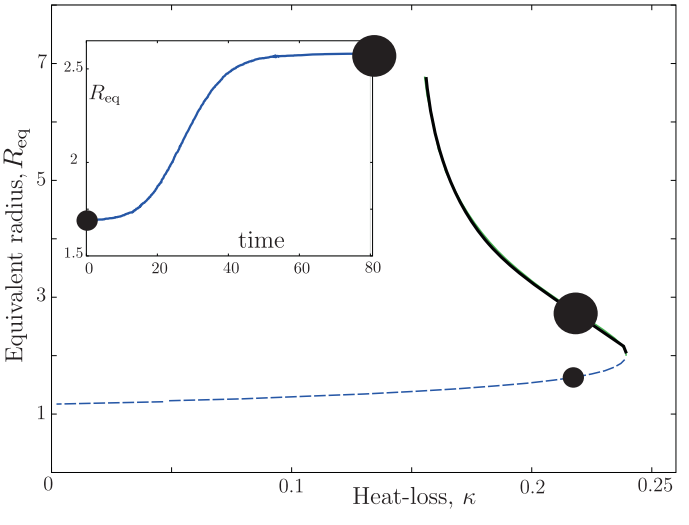

Figure 15. Flame Ball equivalent radius R_{eq} versus heat-loss parameter κ for $l_F = -2$ and $\epsilon_L = 2$. Solid line represents stable solutions. Subfigure: an unstable FB evolving to a larger stable FB ($\kappa = 0.225$).

stable solutions still exist (on the upper branch) for $\epsilon_L = 2$. In the latter case, with relatively large ϵ_L, the lateral boundaries are likely to play an important part in flame stabilisation.

In summary, our numerical results indicate that the flame balls encountered in our mixing layer are typically unstable, as expected for their spherical counterparts, and hence good candidates to incorporate in theories predicting critical ignition conditions. However, we have also shown that they can be stable in special circumstances requiring low Lewis numbers and the presence of heat-losses and depending on the non-uniformity parameter

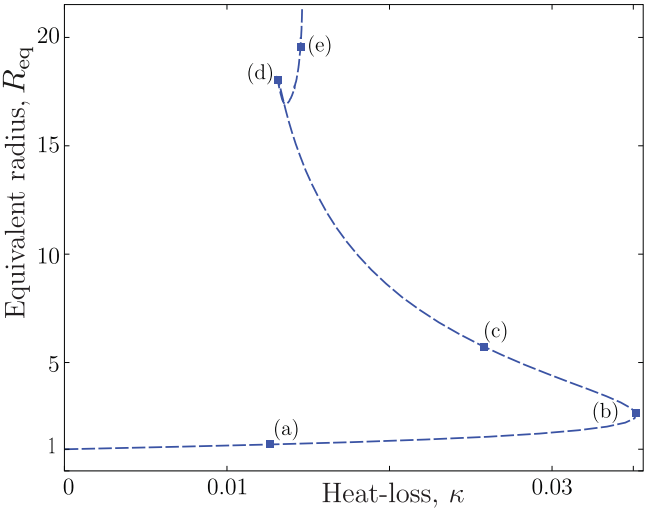

Figure 16. Flame Ball equivalent radius R_{eq} versus heat-loss parameter κ for $l_F = -2$ and $\epsilon_L = 0.5$. All solutions are found to be unstable. The points labelled (a), (b), (c), (d) and (e) refer to the subfigures with the same labelling in Figure 11.

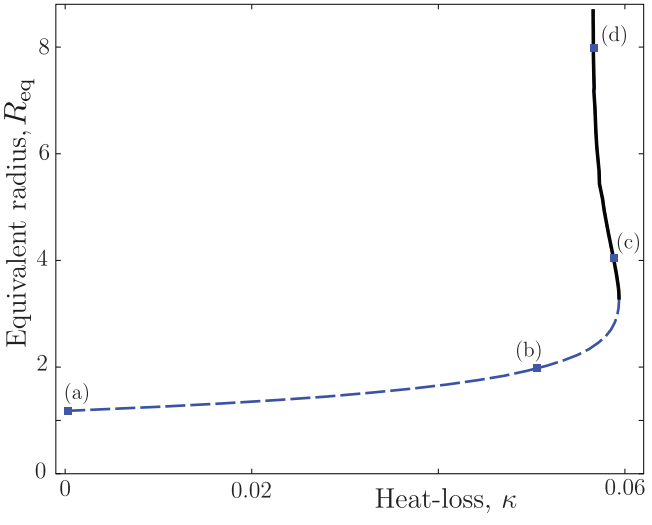

Figure 17. Flame Ball equivalent radius R_{eq} versus heat-loss parameter κ for $l_F = -2$ and $\epsilon_L = 2$. Solid line represents stable solutions. The points labelled (a), (b), (c) and (d) refer to the subfigures with the same labelling in Figure 12.

ϵ_L. It is interesting to note that, at least for the cases identified in Figures 15 and 17, the non-uniformity (that is an increase in the value of ϵ_L) plays a stabilising effect.

5. Conclusions

In this paper, we have significantly expanded our previous treatment of flame balls in mixing layers [1, 2], a subject we believe to be both fundamental for modelling the forced ignition of diffusion flames and important on its own right in combustion theory. Among

the novel contributions of the paper we would like to emphasize (a) the new formulas of section 3.1, elucidating in particular the effect of preferential diffusion on the flame balls, (b) the new free boundary problem (11) involving two dependent variables which models flame balls subject to heat-loss from the burnt gas, (c) the small-ϵ solution of this free boundary problem which leads in particular to formula (28) for the equivalent radius R_{eq} of the distorted flame balls allowing a simple interpretation of the overall effect of a weak mixture's non-uniformity, and (d) the numerical results of section (4) which provide a wealth of information about the existence and stability of the flame balls; we single out in particular the subdivision of the κ-ϵ_L plane for fixed Lewis numbers into four regions which provides useful insight about the modes of burning in the mixing layer including distorted flame balls taking the form of 'flame rings'; we also note the identification of stable flame ball solutions in non-adiabatic low Lewis numbers situations with the non-uniformity parameter ϵ found to play a stabilising role.

Notes

1. In our numerical study, 'near-field losses' are conveniently simulated by taking $H(\theta) = \kappa\theta/\beta$ if $\theta/\theta_{\max} > 1 - 2\beta^{-1}$ and zero otherwise, where $\theta_{\max}$ is the maximum temperature in the domain. Also, 'far-field losses' are simulated by adopting $H(\theta) = \kappa\theta/\beta$ everywhere; in this latter case a better scaled heat loss-model $H(\theta) = \kappa\theta/\beta^2$ could have been adopted [7, 10], but this was not deemed necessary for the numerical study.
2. The non-dimensional coordinates x, y and z are more suitable to the asymptotic analysis (since significant chemical activity is restricted to a strip of thickness of order L/β around the stoichiometric surface [1]) compared to the barred non-dimensional coordinates $\bar{x}$, $\bar{y}$, and $\bar{z}$ (scaled by L) which are more suitable to the numerical analysis as they fix the lateral boundaries of the domain at $\bar{z} = \pm 1$.
3. In the numerical results with finite β presented below, 'near-field heat losses' are simulated conveniently by taking $H(\theta) = \kappa\theta/\beta$ if $\theta/\theta_{\max} > 1 - 2\beta^{-1}$ and zero otherwise, where $\theta_{\max}$ is the maximum temperature in the domain. Numerically, 'far-field heat losses' are also included by adopting $H(\theta) = \kappa\theta/\beta$ everywhere; in this case a better scaled heat loss-model $H(\theta) \propto \theta/\beta^2$ could have been adopted, but this was not deemed necessary.

Disclosure statement

No potential conflict of interest was reported by the authors.

References

[1] J. Daou and R. Daou, *Flame balls in mixing layers*, Combust. Flame 161 (2014), pp. 2015–2024.
[2] R. Daou, P. Pearce, and J. Daou, *Flame balls in non-uniform mixtures: existence and finite activation energy effects*, Combust. Theory Model. 20 (2016), pp. 1–33.
[3] Y.B. Zeldovich, G.I. Barenblatt, V. Librovich, and G.M. Makhviladze, *The Mathematical Theory of Combustion and Explosions*, Consultants Bureau, New York, 1985, p. 327.
[4] B. Zelvovich Ya, *Theory of combustion and detonation of gases*, Izd-vo. Akad. Nauk (Academy of Sciences, USSR), Moscow, 1944.
[5] P.D. Ronney, M.S. Wu, H.G. Pearlman, and K.J. Weiland, *Experimental study of flame balls in space: preliminary results from sts-83*, AIAA J. 36 (1998), pp. 1361–1368.
[6] J. Buckmaster, G. Joulin, and P. Ronney, *The structure and stability of nonadiabatic flame balls*, Combust. Flame 79 (1990), pp. 381–392.
[7] J. Buckmaster, G. Joulin, and P. Ronney, *The structure and stability of nonadiabatic flame balls: II. Effects of far-field losses*, Combust. Flame 84 (1991), pp. 411–422.
[8] C. Lee and J. Buckmaster, *The structure and stability of flame balls: a near-equidiffusional flame analysis*, SIAM. J. Appl. Math. 51 (1991), pp. 1315–1326.

[9] G. Joulin and J. Buckmaster, *Influence of boundary losses on structure and dynamics of flame-balls*, Combust. Sci. Technol. 89 (1984), pp. 57–69(1).
[10] A. Shah, J. Dold, and R. Thatcher, *Stability of a spherical flame ball in a porous medium*, Combust. Theory Model. 4 (2000), pp. 511–534.
[11] J. Daou, F. Al-Malki, and P. Ronney, *Generalized flame balls*, Combust. Theory Model. 13 (2009), pp. 269–294.
[12] A.L. Sánchez and F.A. Williams, *Recent advances in understanding of flammability characteristics of hydrogen*, Prog. Energy Combust. Sci. 41 (2014), pp. 1–55.
[13] E. Fernández-Tarrazo, A.L. Sánchez, A. Liñán, and F.A. Williams, *Flammability conditions for ultra-lean hydrogen premixed combustion based on flame-ball analyses*, Int. J. Hydrogen Energy 37 (2012), pp. 1813–1825.
[14] I. Brailovsky and G. Sivashinsky, *On stationary and travelling flame balls*, Combust. Flame 110 (1997), pp. 524–529.
[15] S. Minaev, L. Kagan, G. Joulin, and G. Sivashinsky, *On self-drifting flame balls*, Combust. Theory Model. 5 (2001), pp. 609–622.
[16] S. Minaev, L. Kagan, and G. Sivashinsky, *Self-propagation of a diffuse combustion spot in premixed gases*, Combust. Explos. Shock Waves 38 (2002), pp. 9–18.
[17] L. Kagan, S. Minaev, and G. Sivashinsky, *On self-drifting flame balls*, Math. Comput. Simul. 65 (2004), pp. 511–520.
[18] J.F. Grcar, *A new type of steady and stable, laminar, premixed flame in ultra-lean, hydrogen–air combustion*, Proc. Combust. Inst. 32 (2009), pp. 1011–1018.
[19] Z. Zhou, *Flame balls at earth gravity*, Ph.D. diss., Technische Universiteit Eindhoven, 2017.
[20] J. Buckmaster and T. Jackson, *Holes in flames, flame isolas, and flame edges*, Proc. Combust. Inst.28 (2000), pp. 1957–1964.
[21] P. Pearce and J. Daou, *Rayleigh–bénard instability generated by a diffusion flame*, J. Fluid. Mech. 736 (2013), pp. 464–494.
[22] P. Pearce and J. Daou, *The effect of gravity and thermal expansion on the propagation of a triple flame in a horizontal channel*, Combust. Flame 160 (2013), pp. 2800–2809.
[23] E. Robert and P.A. Monkewitz, *Experimental realization and characterization of unstretched planar one-dimensional diffusion flames*, Combust. Flame 160 (2013), pp. 546–556.
[24] E. Robert and P.A. Monkewitz, *Thermal-diffusive instabilities in unstretched, planar diffusion flames*, Combust. Flame 159 (2012), pp. 1228–1238.
[25] J. Buckmaster, M. Smooke, and V. Giovangigli, *Analytical and numerical modeling of flame-balls in hydrogen-air mixtures*, Combust. Flame 94 (1993), pp. 113–124.
[26] J. Daou and A. Linán, *The role of unequal diffusivities in ignition and extinction fronts in strained mixing layers*, Combust. Theory Model. 2 (1998), pp. 449–477.
[27] R. Daou, J. Daou, and J. Dold, *Effect of heat-loss on flame-edges in a premixed counterflow*, Combust. Theory Model. 7 (2003), pp. 221–242.
[28] M. Pritulo, *On the determination of uniformly accurate solutions of differential equations by the method of perturbation of coordinates*, J. Appl. Math. Mech. 26 (1962), pp. 661–667.
[29] M.J. Lighthill, *Cix. a technique for rendering approximate solutions to physical problems uniformly valid*, Lond. Edinb. Dublin Philos. Mag. J. Sci. 40 (1949), pp. 1179–1201.
[30] P. Pearce and J. Daou, *Taylor dispersion and thermal expansion effects on flame propagation in a narrow channel*, J. Fluid. Mech. 754 (2014), pp. 161–183.
[31] S. Sohrab, A. Linan, and F. Williams, *Asymptotic theory of diffusion-flame extinction with radiant loss from the flame zone*, Combust. Sci. Technol. 27 (1982), pp. 143–154.
[32] S. James, *Diffusion flame extinction at small stretch rates: the mechanism of radiative loss*, Combust. Flame 65 (1986), pp. 31–34.
[33] F. Liu, G.J. Smallwood, Ö. Gülder, and Y. Ju, *Asymptotic analysis of radiative extinction in counterflow diffusion flames of nonunity lewis numbers*, Combust. Flame 121 (2000), pp. 275–287.
[34] R. Daou, J. Daou, and J. Dold, *Effect of volumetric heat loss on triple-flame propagation*, Proc. Combust. Inst. 29 (2002), pp. 1559–1564.
[35] R. Daou, J. Daou, and J. Dold, *The effect of heat loss on flame edges in a non-premixed counterflow within a thermo-diffusive model*, Combust. Theory Model. 8 (2004), pp. 683–699.